JOURNAL OF SOLID STATE CHEMISTRY **131,** 150–159 (1997)
ARTICLE NO. SC977377

Defect Chemistry of $La_{2-x}Sr_xCuO_{4-\delta}$: Oxygen Nonstoichiometry and Thermodynamic Stability

Hideki Kanai, Junichiro Mizusaki,*,[1] Hiroaki Tagawa, Seiichiro Hoshiyama,†
Katsuhiko Hirano,† Kazuyuki Fujita,‡ Meguru Tezuka,‡ and Takuya Hashimoto§

*Institute of Environmental Science and Technology, Yokohama National University, Tokiwadai, Hodogaya-ku, Yokohama 240, Japan; *Research Institute for Scientific Measurements, Tohoku University, Katahira, Aoba-ku, Sendai 980-77, Japan; †Faculty of Engineering, Shibaura Institute of Technology, Shibaura, Minato-ku, Tokyo 108, Japan; ‡Faculty of Engineering, Saitama Institute of Technology, Fuseiji, Okabe-cho, Ohsato-gun 369-02, Japan; and §Department of Chemistry, College of Arts and Sciences, University of Tokyo, Komaba, Meguro-ku, Tokyo 153, Japan*

Received September 11, 1996; in revised form March 4, 1997; accepted March 5, 1997

The oxygen nonstoichiometry of $La_{2-x}Sr_xCuO_{4-\delta}$ ($x = 0$–0.3) was measured as a function of Sr content, temperature (400–1000°C), and oxygen partial pressure ($P(O_2) = 1$–1×10^{-10} atm) using high-temperature gravimetry and coulometric titration. The oxygen nonstoichiometry ranges from oxygen excess to oxygen deficiency one depending on $P(O_2)$ and the Sr content, x. Oxygen excess was observed for specimens with x less than 0.05. The dependence of oxygen excess nonstoichiometry on oxygen partial pressures was found to be explained by a model with interstitial oxygen as a predominant defect. In oxygen-deficient regions, partial molar enthalpy and partial molar entropy of oxygen were calculated from the nonstoichiometry data. It was revealed from the variation in partial molar enthalpy that a strong interaction between the oxygen and its vacancy exists in oxygen-deficient $La_{2-x}Sr_xCuO_{4-\delta}$. The experimentally obtained partial molar entropy of oxygen was compared with those calculated assuming a so-called metal model, a hopping conduction model, and a narrow band conduction model, where the increase in oxygen vacancies hardly influences the carrier concentration, the holes generated by oxidation of the specimen are trapped by Cu ions, and the holes generated are itinerant, respectively. The variation in partial molar entropy of oxygen could be explained well by either the hopping model or the narrow band conduction model. The oxygen partial pressures required for the decomposition of $La_{2-x}Sr_xCuO_{4-\delta}$ were also measured through the nonstoichiometry measurement. Discontinuity was observed in the dependence of oxygen partial pressures for decomposition on Sr content between $x = 0.05$ and 0.10, suggesting an abrupt variation in the thermodynamic behavior of $La_{2-x}Sr_xCuO_{4-\delta}$ with the Sr content in this region.

1. INTRODUCTION

Since the first discovery of high-T_c superconductivity in the La–Ba–Cu–O system (1), numerous reports have been published on high-T_c superconducting oxides such as $La_{2-x}Sr_xCuO_{4-\delta}$ (2), $Ba_2YCu_3O_{7-\delta}$ (3), and $Bi_2Sr_2Ca_nCu_{n+1}O_{2n+6}$ (4). All the crystal structures of these high T_c superconducting cuprates are so-called perovskite family. Among these, the crystal structure of $La_{2-x}Sr_xCuO_{4-\delta}$ is the simplest K_2NiF_4 type (5). Therefore, $La_{2-x}Sr_xCuO_{4-\delta}$ has often been employed in fundamental studies to elucidate the superconducting mechanism of these cuprates (6).

It has been also reported that the electrical properties of these high-T_c superconductors, such as superconducting transition temperature and electrical conductivity at normal state, are easily affected by oxygen deficiency (7). The effects of oxygen deficiency on the crystal structure and the conduction behavior of $Ba_2YCu_3O_{7-\delta}$ and $Bi_2Sr_2Ca_nCu_{n+1}O_{2n+6}$ were studied by thermogravimetry and so on (8, 9). Several reports have also been published on oxygen deficiency on $La_{2-x}Sr_xCuO_{4-\delta}$. However, there are no reports that contain reliable thermodynamic analysis of the oxygen vacancy and the thermodynamic stability of $La_{2-x}Sr_xCuO_{4-\delta}$. Canerio and co-workers (10) and Serafini and co-workers (11) measured the oxygen nonstoichiometry of $La_{1.8}Sr_{0.2}CuO_{4-\delta}$. They observed a plateau in the oxygen partial pressure, $P(O_2) = 4\times10^{-3}$ atm, in the plots of $P(O_2)$ and δ at 900°C, which could be attributed to impurities segregated in the grain boundaries. Idemoto and Fueki (12) reported the nonstoichiometry of $La_{1.76}Sr_{0.24}CuO_{4-\delta}$ and insisted on a model in which oxygen defects were produced by a single mechanism. That is, the holes generated by oxidation of the specimen are localized in the Cu site, which can be described as

$$O_2 + 2V_O^{\cdot\cdot} + 4Cu_{Cu}^{x} \Leftrightarrow 2O_O^{x} + 4Cu_{Cu}^{\cdot}$$

[1] To whom correspondence should be addressed.

0022-4596/97 $25.00

Here, the Kröger–Vink notation is employed for the expression of defects (13). Opila and Tuller (14) also carried out a thermogravimetric measurement of $La_{2-x}Sr_xCuO_{4-\delta}$ ($x = 0$–1) and insisted on the same mechanism as that of Idemoto and Fueki for the generation of oxygen deficiency. They also claimed that interstitial oxygen existed in Sr-free $La_2CuO_{4\pm\delta}$. However, their analyses are not conclusive since their measurements were carried out in a narrow range of oxygen partial pressures ($\log P(O_2) = 0 - -3.8$) with specimens containing impurities. The oxygen nonstoichiometry of $La_2CuO_{4\pm\delta}$, which did not contain Sr, was also studied by Nishiyama *et al.* (15). They claimed that the defect of $La_2CuO_{4\pm\delta}$ with excess oxygen was either interstitial oxygen in the lattice or a metal vacancy, which could not be distinguished.

In the studies of oxygen nonstoichiometry of $La_{2-x}Sr_xCuO_{4-\delta}$ reported so far, the range of oxygen partial pressures employed was limited to between 1 and 10^{-5} atm and no measurement up to decomposition of $La_{2-x}Sr_xCuO_{4-\delta}$ was reported. Furthermore, there have been few systematic studies of oxygen nonstoichiometry in $La_{2-x}Sr_xCuO_{4-\delta}$ as a function of x, although the Sr content greatly affected the electrical and superconducting properties of $La_{2-x}Sr_xCuO_{4-\delta}$ (16). In this paper, the oxygen nonstoichiometry of $La_{2-x}Sr_xCuO_{4-\delta}$ with $x = 0$, 0.05, 0.10, 0.16, 0.20, and 0.30 is reported. The amount of oxygen deficiency, δ, was measured as a function of temperature, T, in the range 400–1000°C and of $P(O_2)$ in the range 1–10^{-10} atm, using a microthermobalance, coulometric titration, and iodometry. In the $P(O_2)$ range employed in this study, decomposition of the specimens is observed and the thermodynamic stability of $La_{2-x}Sr_xCuO_{4-\delta}$ is discussed. The defect formation mechanism is also discussed using a partial molar enthalpy and entropy of oxygen calculated from the observed oxygen nonstoichiometry. The relationship between oxygen deficiency and the electrical properties of $La_{2-x}Sr_xCuO_{4-\delta}$ will be discussed in separate papers (17, 18).

2. EXPERIMENTAL

2.1. Sample Preparation

The samples were prepared from mixtures of La_2O_3 (99.9%), $SrCO_3$ (99.9%), and CuO (99.9%) by solid state reaction. Prior to mixture, La_2O_3 was annealed at 1000°C for 3 h in air to decompose impurities such as $La(OH)_3$ and $La_2(CO_3)_3$. $SrCO_3$ was dried in air at 150°C to remove adsorbed water. CuO was annealed at 800°C for more than 24 h under 1 atm of $P(O_2)$ and cooled slowly to room temperature to make a copper valence of $2+$. After determination of their factors by iodometric titration, the oxides and carbonate were mixed at a nominal ratio. The mixture was calcined at 900°C for about 10 h and then heated at 1000°C for 12 h. The powder sample obtained was confirmed to have a single-phase K_2NiF_4-type structure by X-ray diffraction. The powders sample was pressed into pellets at 10^3 kg/cm^2 and sintered at a temperature from 1050 to 1200°C for 3 h. Cation content of the sintered pellets was measured by SEM-EDX. The measured cation content agreed with the prescribed ratio within $\Delta x = \pm 0.02$. The density of pellets used for the nonstoichiometry measurement was about 70%.

2.2. Measurement of Oxygen Nonstoichiometry

Two methods were employed for measurement of the oxygen nonstoichiometry of $La_{2-x}Sr_xCuO_{4-\delta}$: thermogravimetry and coulometric titration were used in the ranges $1\,\text{atm} \geq P(O_2) \geq 10^{-5}$ atm and $10^{-4}\,\text{atm} \geq P(O_2) \geq 10^{-10}$ atm, respectively. Thermogravimetry was not used at the lower oxygen partial pressures because the equilibrium state would not be realized due to the slow rate of reaction between the gas phase and the specimen. Coulometric titration was not used in the higher oxygen partial pressures since analysis of the data was not simple in that range. The absolute value of oxygen deficiency was determined by thermodynamic analyses of $P(O_2)$–T–δ relationships and confirmed by iodometric titration.

2.2.1. Thermogravimetry. A gas flow-type thermobalance (CAHN1000) was used for the measurement in the temperature range from 400 to 1000°C and in the $P(O_2)$ range from 1 to 10^{-4} atm. The $P(O_2)$ was controlled by mixing O_2 and Ar gas and monitored by a zirconia oxygen sensor. The weight at equilibrium state at the specified temperature and oxygen partial pressure was measured. The amount of oxygen deficiency, δ, was calculated from the weight variation, assuming that it was caused only by the variation of oxygen nonstoichiometry in the specimen.

2.2.2. Coulometric titration. The oxygen nonstoichiometry of $La_{2-x}Sr_xCuO_{4-\delta}$ under the oxygen partial pressures below 10^{-3} atm was measured by coulometric titration using a zirconia tube (19). Figure 1 shows a schematic diagram of an apparatus for the coulometric titration.

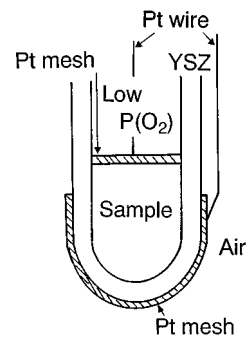

FIG. 1. Schematic diagram of the apparatus for coulometric titration.

A platinum paste was painted on the outside of the tube, which was baked at 900°C for 2 h to prepare the electrode. A piece of sintered sample was weighed, placed inside the tube, and pulverized with slight pressure so that the powdered sample was in close contact with the tube wall. A platinum mesh was attached to the powder sample as the other electrode by mechanical pressure. Platinum wires were employed as leads. The inside of the tube was then evacuated and refilled with Ar gas. The pressure of Ar gas was kept at about 10 mm Hg at room temperature to prevent the influence of residual oxygen and to realize the equilibrium state quickly. After the temperature was raised to 800–1000°C, voltage was applied so that oxygen ions could flow from the inside to the outside of the tube. The amount of oxygen to be extracted from the sample was controlled by the quantity of electricity passed through the cell. After a specified quantity of electricity was used, the electromotive force between the inside and the outside of the tube was measured to calculate the equilibrium oxygen partial pressure inside the tube. Under the condition that the amount of oxygen inside the tube was negligibly small compared with the oxygen deficiency of the specimen, i.e., $P(O_2) < 10^{-3}$ atm, the amount of oxygen deficiency, δ, was calculated using the equation

$$\delta = C/(2MF).$$

Here, C, M, and F represent the quantity of electricity, the amount of the sample in moles, and the Faraday constant, respectively.

2.2.3. Iodometric titration. The $La_{2-x}Sr_xCuO_{4-\delta}$ pellet was annealed at 800°C under 1 atm of oxygen for more than 30 h. After an equilibrium state was realized, the sample was quenched to a water-cooled temperature by a method similar to that in (20). An appropriate amount of the sample was dissolved in an HCl solution containing KI. I_2 was liberated by the reactions

$$2Cu^{2+} + 4I^- \rightarrow 2CuI + I_2$$

$$2Cu^{3+} + 6I^- \rightarrow 2CuI + 2I_2.$$

The concentration of I_2 was determined with 0.1 N $Na_2S_2O_3$ and the oxygen concentration was calculated (21).

3. RESULTS

Figure 2 shows the dependence of oxygen content on log $P(O_2)$ of $La_2CuO_{4\pm\delta}$. Relationships of downward convex curves were observed between oxygen content and oxygen partial pressures, suggesting that the oxygen content was hyperstoichiometric, i.e., more than 4, At low $P(O_2)$, oxygen content gradually reached a constant value and

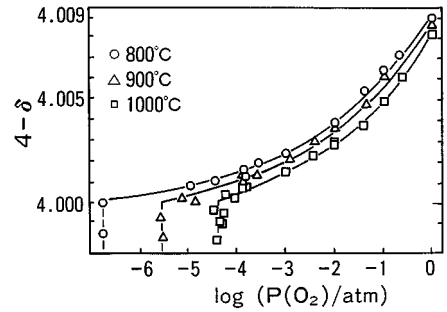

FIG. 2. Dependence of oxygen content of $La_2CuO_{4-\delta}$ on log $P(O_2)$ at 800–1000°C. Dashed lines represent log $P(O_2)$ for the decomposition of the specimen.

a plateau was observed in the relationship between δ and log $P(O_2)$. According to Wagner (22), the slope of the δ vs log $P(O_2)$ plot shows a minimum at the point of the stoichiometric composition. Therefore, the oxygen content at the plateau was determined to be 4.000.

The iodometric titration of $La_2CuO_{4\pm\delta}$ annealed at 800°C at $P(O_2)$ of 1 atm was carried out to confirm the oxygen content. Table 1 lists the results. The oxygen content determined by iodometry agrees with the data from thermogravimetry within experimental error. Also observed were the log $P(O_2)$ values for the decomposition of $La_2CuO_{4\pm\delta}$, indicated by dashed lines in Fig. 2.

Figure 3 shows the relationship of oxygen content to log $P(O_2)$ of $La_{1.95}Sr_{0.05}CuO_{4-\delta}$. The oxygen content at the plateau observed at 1000°C and $0 \geq \log P(O_2) \geq -1.5$ was determined to be 4.000, which was confirmed by iodometry as Table 1 lists. A hyperstoichiometric region was observed at 800°C in the whole $P(O_2)$ range and at 900°C in the log $P(O_2)$ range above -4.4, while a hypostoichiometric region was found in the log $P(O_2)$ range below -4.4 at 900°C and in the entire log $P(O_2)$ range at 1000°C. Dashed lines in Fig. 3 represent log $P(O_2)$ for the decomposition of the specimens.

TABLE 1
Oxygen Content of the Specimens Determined by Thermogravimetry and Iodometry

Sample	Oxygen content determined by	
	Thermogravimetry	Iodometry
$La_2CuO_{4\pm\delta}$	4.009	4.005 ± 0.004
$La_{1.95}Sr_{0.05}CuO_{4\pm\delta}$	4.003	4.004 ± 0.003
$La_{1.90}Sr_{0.10}CuO_{4-\delta}$	4.000	4.002 ± 0.003
$La_{1.84}Sr_{0.16}CuO_{4-\delta}$	4.000	4.000 ± 0.003
$La_{1.80}Sr_{0.20}CuO_{4-\delta}$	3.993	3.995 ± 0.004
$La_{1.70}Sr_{0.30}CuO_{4-\delta}$	3.983	3.985 ± 0.004

Note. The specimens were annealed at 800°C under 1 atm of oxygen.

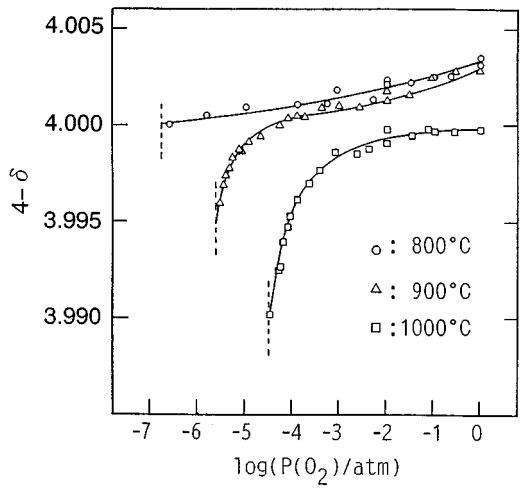

FIG. 3. Dependence of oxygen content of $La_{1.95}Sr_{0.05}CuO_{4-\delta}$ on $\log P(O_2)$ at 800–1000°C. Dashed lines represent $\log P(O_2)$ for the decomposition of the specimen.

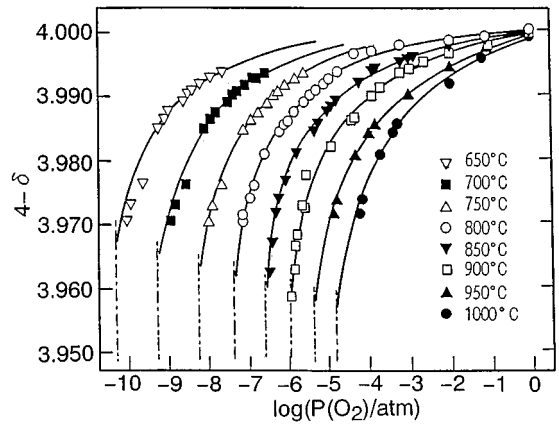

FIG. 5. Dependence of oxygen content of $La_{1.84}Sr_{0.16}CuO_{4-\delta}$ on $\log P(O_2)$ at 650–1000°C. Dashed lines represent $\log P(O_2)$ for the decomposition of the specimen.

Figures 4, 5, 6, and 7 show the dependence of oxygen content on oxygen partial pressures $La_{2-x}Sr_xCuO_{4-\delta}$ with $x = 0.10$, 0.16, 0.20, and 0.30, respectively. In every specimen, the oxygen content of the specimen decreased as the temperature increased and as the oxygen partial pressure decreased. No discontinuity, such as was detected in the δ vs $\log P(O_2)$ curve of the specimen containing impurities (10, 11), was observed in Figs. 4–7. Downward convex relationships between the oxygen content and the oxygen partial pressures were not observed but upward convex relationships were detected. This showed that not oxygen excess but oxygen deficiency nonstoichiometry was stable in $La_{2-x}Sr_xCuO_{4-\delta}$ with $x \geq 0.10$ under the measurement conditions. The oxygen content at the plateau in Figs. 4–7 was determined to be 4.000 by Wagner's theory (22), which was also confirmed by iodometry as listed in Table 1. The decomposition of the specimens was observed below the $\log P(O_2)$ indicated by dashed lines in Figs. 4–7.

Figure 8 shows relationships between the oxygen content and the oxygen partial pressure of $La_{2-x}Sr_xCuO_{4-\delta}$ at 900°C. Hyperstoichiometric and hypostoichiometric regions were observed at Sr content below $x \leq 0.05$ and $x \geq 0.10$, respectively. A plateau was observed at stoichiometric composition with $x = 0.10$. The amount of oxygen deficiency, δ, increased with the increase in the Sr content and the decrease in the oxygen partial pressure at a constant temperature.

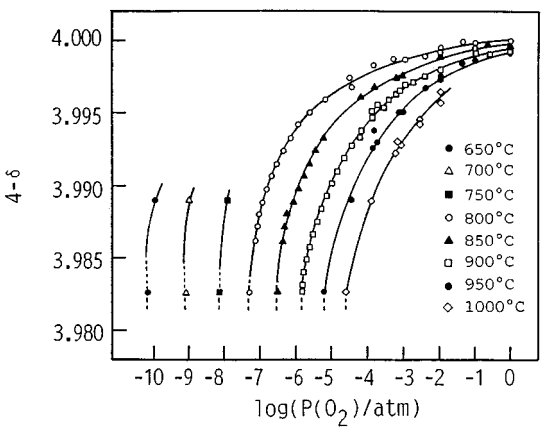

FIG. 4. Dependence of oxygen content of $La_{1.90}Sr_{0.10}CuO_{4-\delta}$ on $\log P(O_2)$ at 650–1000°C. Dashed lines represent $\log P(O_2)$ for the decomposition of the specimen.

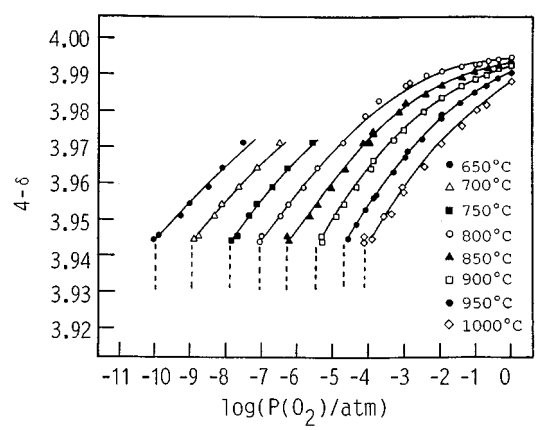

FIG. 6. Dependence of oxygen content of $La_{1.80}Sr_{0.20}CuO_{4-\delta}$ on $\log P(O_2)$ at 650–1000°C. Dashed lines represent $\log P(O_2)$ for the decomposition of the specimen.

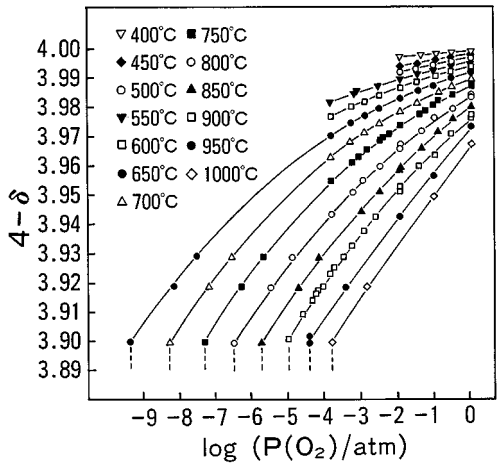

FIG. 7. Dependence of oxygen content of $La_{1.70}Sr_{0.30}CuO_{4-\delta}$ on $\log P(O_2)$ at 400–1000°C. Dashed lines represent $\log P(O_2)$ for the decomposition of the specimen.

4. DISCUSSION

In an analysis of defect structures of $La_{2-x}Sr_xCuO_{4-\delta}$, the oxygen nonstoichiometry data were considered from the viewpoint of the thermodynamics of defect equilibrium. Two regions, one with excess oxygen of $x = 0$ and 0.05 and the other with oxygen deficiency of $x = 0.05$–0.30, were distinguished. Also thermodynamically considered was the thermodynamics of decomposition of $La_{2-x}Sr_xCuO_{4-\delta}$.

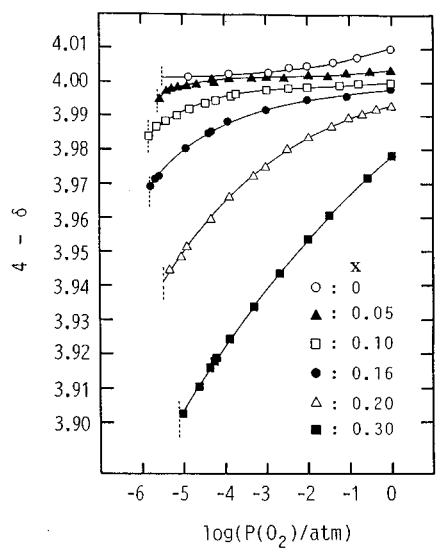

FIG. 8. Oxygen content of $La_{2-x}Sr_xCuO_{4-\delta}$ as a function of oxygen partial pressure at 900°C. Greater oxygen deficiency was observed at higher Sr content, x.

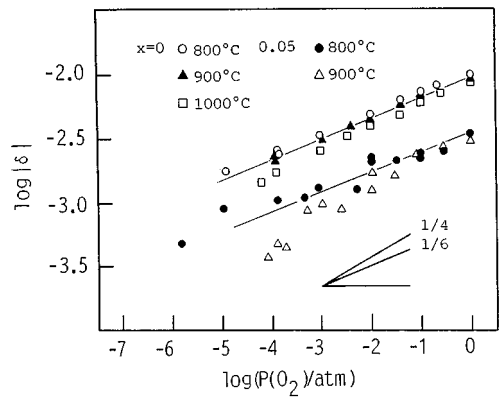

FIG. 9. $\log|\delta|$ vs $\log P(O_2)$ plot for $La_2CuO_{4-\delta}$ and $La_{1.95}Sr_{0.05}CuO_{4-\delta}$ in the hyperstoichiometric region. Almost linear relationships with a proportionality constant of about 1/6 were observed.

4.1. Defects in the Hyperstoichiometric Region

Figure 9 shows the relationships between $\log|\delta|$ and $\log P(O_2)$ for $La_2CuO_{4-\delta}$ and $La_{1.95}Sr_{0.05}CuO_{4-\delta}$ in the hyperstoichiometric region. In both specimens, an almost linear relationship with a proportionality constant of about 1/6 was observed, although deviations due to large experimental error were observed for the specimen with $x = 0.05$ in the $\log P(O_2)$ range below -2. Considering that the electric carrier is a hole in both specimens (23), two kinds of defects, a metal vacancy and interstitial oxygen, can be considered.

Assuming that the metal vacancy is the predominant defect, the defect equilibrium can be written as

$$1/2O_2(g) \Leftrightarrow O_o^x + 1/4V''_{Cu} + 1/2V'''_{La} + 2Cu^{\bullet}_{Cu}.$$

Here, O_o^x, V''_{Cu}, V'''_{La}, and $Cu^{\bullet}_{Cu}$ represent an oxygen ion at the oxygen site in the crystal lattice, a doubly negatively charged Cu vacancy, a triply negatively charged La vacancy, and a positively charged Cu ion at the Cu site (normally Cu^{2+}) in the crystal lattice, respectively. If a quasichemical mass action law is satisfied,

$$K = [O_o^x][V''_{Cu}]^{1/4}[V'''_{La}]^{1/2}[Cu^{\bullet}_{Cu}]^2/P(O_2)^{1/2} \qquad [1]$$

where K is the equilibrium constant. Here, the electrical neutrality condition for the semiconductor model is expressed as

$$[Cu^{\bullet}_{Cu}] = 2[V''_{Cu}] + 3[V'''_{La}]. \qquad [2]$$

By substitution of Eq. [2] into Eq. [1], we can obtain the relation

$$\delta \propto [V'''_{La}] \propto P(O_2)^{2/11}. \qquad [3]$$

That is, defect concentration is proportional to the 1/5.5 power of oxygen partial pressure.

In the case where interstitial oxygen is assumed to be the predominant defect, the defect equilibrium can be expressed as

$$1/2O_2(g) \Leftrightarrow O_i'' + 2Cu_{Cu}^{\bullet}.$$

Here, O_i'' denotes doubly negatively charged interstitial oxygen. The quasichemical mass action law of the above defect equilibrium can be expressed as

$$K = [O_i''][Cu_{Cu}^{\bullet}]^2/P(O_2)^{1/2} \qquad [4]$$

where K is the equilibrium constant. The electrical neutrality condition for the semiconductor model can be expressed as

$$2[O_i''] = [Cu_{Cu}^{\bullet}]. \qquad [5]$$

Substituting Eq. [5] into Eq. [4], we can obtain the relationship

$$\delta \propto [O_i''] \propto P(O_2)^{1/6}. \qquad [6]$$

Thus, the defect concentration is proportional to the 1/6 power of oxygen partial pressure.

Due to experimental error, whether the slope of Fig. 9 is 1/6 or 1/5.5 cannot be determined. However, we suppose that the predominant defect in the hyperstoichiometric region of $La_{2-x}Sr_xCuO_{4-\delta}$ would be interstitial oxygen rather than the metal vacancy. From neutron diffraction of powdered $La_2CuO_{4.032}$ prepared at 600°C in 1–3 kbar O_2, Chillout *et al.* found that interstitial oxygen entered into the rock salt layer (24). This result is qualitatively in good agreement with our thermogravimetric results. The amount of excess oxygen in our measured temperature and $\log P(O_2)$ range is so small that it cannot be distinguished in $La_2CuO_{4\pm\delta}$ prepared under O_2 or reduced atmosphere by neutron diffraction study (25).

4.2. Defects in the Hypostoichiometric Region

In this section, the defect model for the oxygen-deficient region is discussed. Figure 10 shows relationships between $\log\delta$ and $\log P(O_2)$ of the specimens with oxygen deficiency. In the $\log P(O_2)$ region above -2, an almost linear relationship with a proportionality constant of about $-1/2$ was observed in every specimen. In this region, the defect equilibrium can be expressed as

$$1/2O_2 + V_o^{\bullet\bullet} \Leftrightarrow O_o^x + 2h^{\bullet}.$$

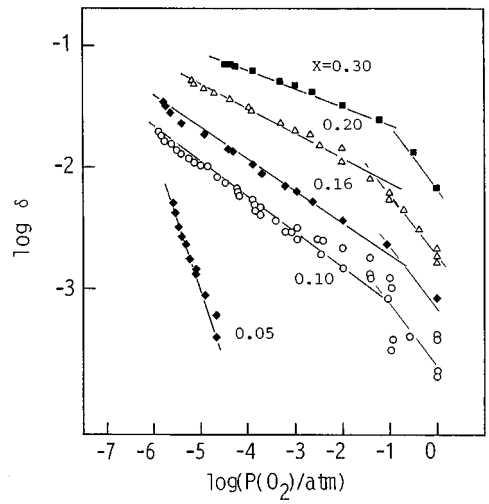

FIG. 10. $\log\delta$ vs $\log P(O_2)$ for $La_{2-x}Sr_xCuO_{4-\delta}$ in the hypostochiometric region at 900°C.

Here, $V_o^{\bullet\bullet}$ and $h^{\bullet}$ represent a doubly negatively charged oxygen vacancy and a positively charged itinerant hole, respectively. The quasichemical mass action law can be expressed as

$$K = [h^{\bullet}]^2/([V_o^{\bullet\bullet}]P(O_2)^{1/2}), \qquad [7]$$

where K is the equilibrium constant. The electrical neutrality condition can be expressed as

$$[h^{\bullet}] + 2[V_o^{\bullet\bullet}] = [Sr_{La}']. \qquad [8]$$

In this region, Eq. [8] can be approximated as

$$[h^{\bullet}] = [Sr_{La}'] \qquad [9]$$

because of the small amount of δ. By substitution of Eq. [9] into Eq. [7], we obtain the relation

$$\delta = [V_o^{\bullet\bullet}] \propto P(O_2)^{-1/2}.$$

In the $\log P(O_2)$ region below -2 where the number of oxygen vacancies increases, almost linear relationships between $\log\delta$ and $\log P(O_2)$ were also observed; however, the proportionality constant gradually increased with increased Sr content from about -1 at $x = 0.05$ to about $-1/6$ at $x = 0.30$. This behavior resembles that of the oxygen deficiency of $La_{1-x}Sr_xCoO_{3-\delta}$, to which an analysis of defects based on the simple semiconductor model cannot be applied (26). Therefore, we concluded that a simple defect model such as that applied in the hyperstoichiometric region of $La_2CuO_{4\pm\delta}$ was not appropriate in the hypostoichiometric region of $La_{2-x}Sr_xCuO_{4-\delta}$. Accordingly, the

variation in oxygen partial molar enthalpy, ΔH_o, and that in oxygen partial molar entropy, ΔS_o, were analyzed. ΔH_o and ΔS_o were calculated from the data depicted in Figs. 2–7 using the equations (27)

$$\Delta H_o = \{\partial(\Delta\mu_{o(s)}/T)/\partial(1/T)\}_P$$
$$= 1/2\{\partial(R\ln P(O_2))/\partial(1/T)\}_P$$
$$\Delta S_o = -\{\partial(\Delta\mu_{o(s)})/\partial T\}_P$$
$$= -1/2\{\partial(RT\ln P(O_2))/\partial T\}_P,$$

where $\Delta\mu_{o(s)}$ denotes the chemical potential of oxygen in solids at 1 atm. ΔH_o and ΔS_o for a specimen with specified δ can be calculated from the inclination of the plots of $R\ln P(O_2)$ vs $1/T$ and $RT\ln P(O_2)$ vs T, respectively.

Figures 11 and 12 show the relationship between δ and calculated ΔH_o and ΔS_o, respectively. A discontinuity in the behavior of ΔH_o and ΔS_o, was observed between the hyperstoichiometric and hypostoichiometric regions, suggesting different mechanisms for generation of oxygen defects in the two regions. In the hypostoichiometric region, ΔH_o increased with the increase in x, in good agreement with the increase in δ with increased x as shown in Fig. 8. The insets of Figs. 11 and 12 show ΔH_o and ΔS_o calculated from the nonstoichiometry data of the hypostoichiometric region, respectively. It was observed that ΔH_o depends on both x and δ. In the region where δ was smaller than 0.03, the relationship between ΔH_o and δ could not be clarified due to large experimental error. However, almost linear relationships were observed between ΔH_o and δ in the region where δ was larger than 0.03, indicating that the thermodynamic behavior of the oxygen vacancy in the large δ region is like that of a regular solution rather than that of an ideal solution. In other words, the vacancy–oxygen interaction is stronger than the mean value of vacancy–vacancy and oxygen–oxygen interaction.

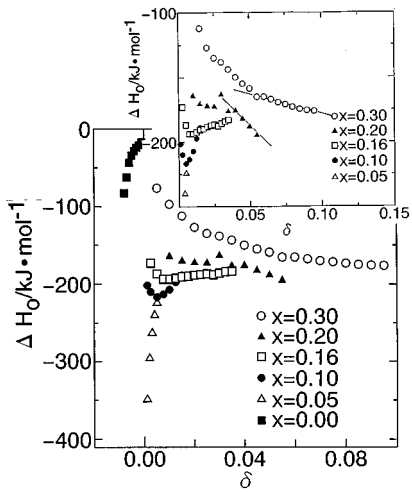

FIG. 11. Partial molar enthalpy of oxygen, ΔH_o, calculated from nonstoichiometry data. A difference in the behavior of ΔH_o was observed between the hyperstoichiometric and hypostoichiometric regions. ΔH_o increases as x increases in the hypostoichiometric region. The inset shows the dependence of ΔH_o on oxygen deficiency in the hypostoichiometric region. The transverse axis is enlarged. A nearly linear relationship was observed at large δ.

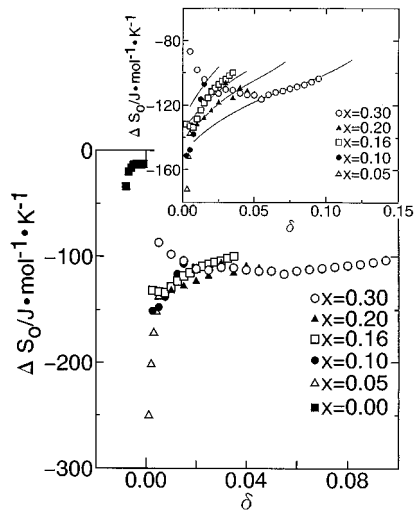

FIG. 12. Partial molar entropy of oxygen, ΔS_o, calculated from nonstoichiometry data. A difference in the behavior of ΔS_o was observed between the hyperstoichiometric and hypostoichiometric regions. The inset shows the dependence of ΔS_o on oxygen deficiency in the hypostoichiometric region. Solid curves reprersent ΔS_o (config.) curve fitting results calculated using the hopping or narrow band conduction model, explained in the text.

Although ΔS_o of the specimens with large x and small δ included large errors, it increased with the increase in δ where δ was large enough. Here, the configuration entropy of oxygen, ΔS_o (config.), which could be calculated from the various defect models, was compared with the experimentally obtained ΔS_o. The partial molar entropy of oxygen, ΔS_o, is the summation of the vibration partial molar entropy of oxygen, ΔS_o (vib.), and the configuration partial molar entropy of oxygen, ΔS_o (config.). When continuous change in oxygen nonstoichiometry, δ, is observed in the same phase and the same defect equilibrium is realized, ΔS_o should be described by the configuration entropy of oxygen, ΔS_o (config.), since the term ΔS_o (vib.) hardly changes (28).

At first, a so-called metal model, where oxygen vacancies were randomly distributed and did not influence the concentration of the electron carrier, was assumed. The defect equilibrium can be expressed as

$$1/2O_2 + V_o^{\cdot\cdot} \Leftrightarrow O_o^x + 2h^{\cdot}.$$

The quasichemical mass action law can be expressed as

$$K = ([O_o^x][h^\bullet]^2)/([V_o^{\bullet\bullet}]P(O_2)^{1/2})\cdot \cdot(\gamma(O_o^x)\gamma(h^\bullet)^2)/(\gamma(V_o^{\bullet\bullet})\gamma(O_2)^{1/2}). \quad [10]$$

K and γ represent the equilibrium constant and the activity coefficient, respectively. In the metal model $[h^\bullet]$ can be regarded as a constant because it is independent of oxygen deficiency. Thus, K can be described as

$$K = C\{(4-\delta)/\delta\}P(O_2)^{-1/2}, \quad [11]$$

where C is a product of $[h^\bullet]^2$ and $(\gamma(O_o^x)\gamma(h^\bullet)^2)/(\gamma(V_o^{\bullet\bullet})\gamma(O_2)^{1/2})$, which can be regarded as a constant. Since the variation in Gibbs free energy, ΔG, can be expressed in terms of the equilibrium constant, K, as

$$\Delta G = -RT\ln K, \quad [12]$$

ΔG can be written as

$$\Delta G = -RT\ln P(O_2)^{-1/2} - RT\ln\{(4-\delta)/\delta\} - RT\ln C. \quad [13]$$

The second term on the right side of Eq. [13] corresponds to the configuration partial molar entropy; therefore, ΔS_o (config.) can be expressed as

$$\Delta S_o(\text{config.}) = -R\ln\{(4-\delta)/\delta\}. \quad [14]$$

The dependence of ΔS_o (config.) on δ calculated by this equation is shown in Fig. 13a.

Next, ΔS_o (config.) was calculated using a hopping conduction model, where oxygen vacancies were positively charged and holes generated by oxidation of the specimens were trapped by Cu ions. The defect equilibrium can be expressed as

$$1/2O_2 + V_o^{\bullet\bullet} + 2Cu_{Cu}^x \Leftrightarrow O_o^x + 2Cu_{Cu}^\bullet.$$

Here, Cu_{Cu}^x indicates an electrically neutral Cu atom in the Cu site in the crystal lattice. The quasichemical mass action law is expressed as

$$K = ([O_o^x][Cu_{Cu}^\bullet]^2)/([V_o^{\bullet\bullet}][Cu_{Cu}^x]^2P(O_2)^{1/2}) \cdot(\gamma(O_o^x)\gamma(Cu_{Cu}^\bullet)^2)/(\gamma(V_o^{\bullet\bullet})\gamma(Cu_{Cu}^x)^2\gamma(O_2)^{1/2}). \quad [15]$$

The electrical neutral condition is described by the formula

$$[Sr'_{La}] = [Cu_{Cu}^\bullet] + 2[V_o^{\bullet\bullet}]. \quad [16]$$

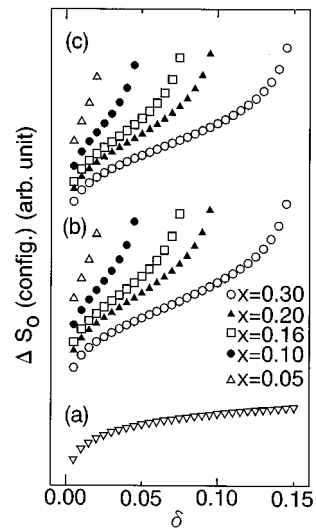

FIG. 13. Calculated results of ΔS_o (config.) based on the metal model (a), the hopping conduction model (b), and the narrow band conduction model (c).

Since $[Sr'_{La}] = x$, $[V_o^{\bullet\bullet}] = \delta$ and $[Cu_{Cu}^\bullet] + [Cu_{Cu}^x] = 1$, the following equations can be derived from Eq. [16]:

$$[Cu_{Cu}^x] = 1 + 2\delta - x \quad [17]$$

$$[Cu_{Cu}^\bullet] = x - 2\delta. \quad [18]$$

By substitution of Eqs. [17] and [18] into Eq. [15], the equilibrium constant, K, can be written as

$$K = \{(4-\delta)/\delta\}\cdot\{(x-2\delta)/(1+2\delta-x)\}^2P(O_2)^{-1/2}\cdot\pi(\gamma). \quad [19]$$

Here, $\pi(\gamma)$ is equal to $(\gamma(O_o^x)\gamma(Cu_{Cu}^\bullet)^2)/(\gamma(V_o^{\bullet\bullet})\gamma(Cu_{Cu}^x)^2\gamma(O_2)^{1/2})$. By carrying out a calculation similar to that of the metal model, ΔS_o (config.) can be expressed as

$$\Delta S_o(\text{config.}) = -R\ln\{(4-\delta)/\delta\}\{(x-2\delta)/(1+2\delta-x)\}^2. \quad [20]$$

The dependence of ΔS_o (config.) on δ, calculated using Eq. [20] is shown in Fig. 13b.

Third, a narrow band conduction model was employed for the calculation of ΔS_o (config.). In this model, itinerant holes can be generated by oxidation of the specimens in a conduction band with narrow dispersion. Semimetallic conduction behavior can be expected since mobility of the generated hole should be lower than that in metals. The defect equilibrium was expressed as

$$1/2O_2 + V_o^{\bullet\bullet} \Leftrightarrow O_o^x + 2h^\bullet.$$

The quasichemical mass action law can be expressed as

$$K = ([O_o^x][h^\cdot]^2)/([V_o^{\cdot\cdot}]P(O_2)^{1/2}) \cdot (\gamma(O_o^x)\gamma(h^\cdot)^2)/(\gamma(V_o^{\cdot\cdot})\gamma(O_2)^{1/2}). \quad [21]$$

The electrical neutrality condition is expressed as

$$[Sr'_{La}] = [h^\cdot] + 2[V_o^{\cdot\cdot}]. \quad [22]$$

Since $[Sr'_{La}] = x$ and $[V_o^{\cdot\cdot}] = \delta$,

$$[h^\cdot] = x - 2\delta. \quad [23]$$

Therefore, the equilibrium constant, K, is expressed as

$$K = \{(4-\delta)/\delta\}(x-2\delta)^2 P(O_2)^{-1/2} \cdot \pi(\gamma), \quad [24]$$

where $\pi(\gamma) = (\gamma(O_o^x)\gamma(h^\cdot)^2)/(\gamma(V_o^{\cdot\cdot})\gamma(O_2)^{1/2})$. Therefore, the next equation for ΔS_o (config.) can be obtained:

$$\Delta S_o(\text{config.}) = -R\ln\{(4-\delta)/\delta\}(x-2\delta)^2. \quad [25]$$

Figure 13c shows results of calculation using Eq. [25].

Comparison of Fig. 13 with the inset of Fig. 12 revealed that the metal model was not appropriate for explanation of the dependence of ΔS_o (config.) on δ since ΔS_o (config.) depended on both x and δ. In addition, nearly constant ΔS_o (config.) should be observed at a higher δ region for the metal model, in disagreement with the experimental results. Dependence of observed ΔS_o (config.) on δ and x showed fairly good correspondence with ΔS_o (config.) calculated using a hopping or narrow band conduction model, as shown in the solid curves in the inset of Fig. 12. However, whether holes generated by oxidation of the specimens were trapped or itinerant could not be determined since the calculated results were almost the same with both models. Measurements of the electrical transport would be required for the determination of behavior of the holes; these measurements will be presented in a separate paper (17).

4.3. Temperature Dependence of Oxygen Partial Pressure for Decomposition of $La_{2-x}Sr_xCuO_{4-\delta}$

Oxygen partial pressure for decomposition $La_{2-x}Sr_xCuO_{4-\delta}$ was determined by coulometric titration and is indicated by a dashed line in Figs. 2–7. The dependence of oxygen partial pressure for decomposition of $La_{2-x}Sr_xCuO_{4-\delta}$ on the reciprocal of the temperature is shown in Fig. 14. A linear relationship whose slope was affected by the variation in enthalpy for the decomposition was observed for each specimen; however, the specimens with $x = 0$ and 0.05 and those with $x = 0.10$, 0.16, 0.20, and 0.30 showed different slopes. Figure 15 shows variations in oxygen partial pressure for the decomposition with Sr content at 700–1000°C. The oxygen partial pressure for decomposition was nearly independent of Sr content for the specimen with $x \leq 0.05$. However, it increased with increased Sr content for $La_{2-x}Sr_xCuO_{4-\delta}$ with $x \geq 0.10$, showing correspondence with the increase in Cu mean valence. A discontinuity was observed in the dependence of the oxygen partial pressure for decomposition on the Sr content between the specimens with $x = 0.05$ and $x = 0.10$, suggesting a difference in thermodynamic behavior.

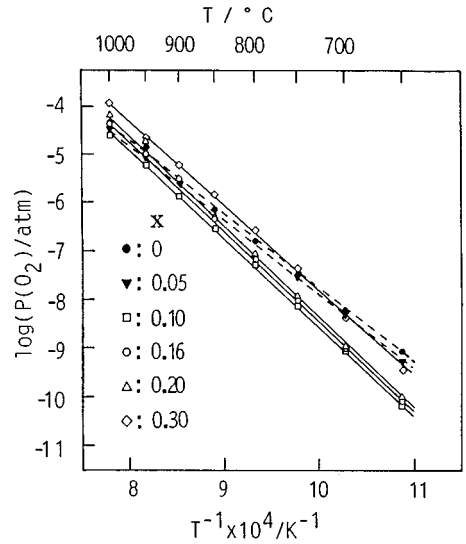

FIG. 14. Dependence of $\log P(O_2)$ for decomposition of the specimens on the reciprocal of temperature. Linear relationships were observed.

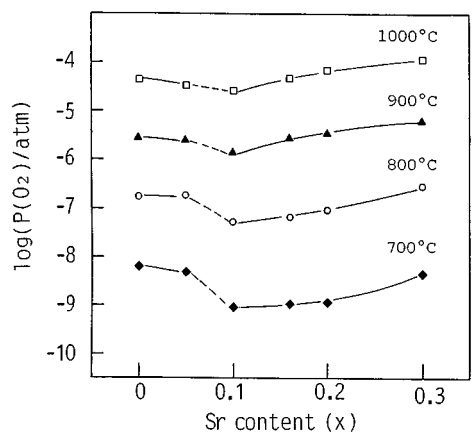

FIG. 15. Variation of oxygen partial pressure for decomposition of $La_{2-x}Sr_xCuO_{4-\delta}$ on Sr content at 700–1000°C.

5. CONCLUSION

(1) The dependence of the oxygen nonstoichiometry of $La_{2-x}Sr_xCuO_{4-\delta}$ on oxygen partial pressure and temperature was determined by thermogravimetry and coulometric titration. $La_{2-x}Sr_xCuO_{4-\delta}$ with $x = 0$ to 0.05 shows oxygen excess nonstoichiometry, whereas that with x greater than 0.10 shows only an oxygen-deficient region.

(2) In the oxygen hyperstoichiometric region, interstitial oxygen is more probable than metal vacancy as a predominant defect, since the relationships between $\log|\delta|$ and $\log P(O_2)$ could be better explained by the interstitial oxygen model. This consideration agrees well with the results of neutron diffraction study.

(3) In the oxygen-deficient region, the configuration entropy of oxygen could be explained either by the hopping or by the narrow band conduction model but not by the metal model. Whether the holes generated by oxidation were localized around Cu ions or were itinerant could not be determined by thermogravimetric measurement only.

(4) In the dependence of the oxygen partial pressure for the decomposition of $La_{2-x}Sr_xCuO_{4-\delta}$ on the Sr content, a discontinuity was observed between the specimens with $x \leq 0.05$ and those with $x \geq 0.10$. Abrupt variation in the thermodynamic behavior of $La_{2-x}Sr_xCuO_{4-\delta}$ in the region between $x = 0.05$ and 0.10 was suggested.

ACKNOWLEDGMENT

This work was partly supported by a Grant-in-Aid for Scientific Research on Priority Areas (No. 260: Dynamics of Fast Ions in Solid and Its Evolution for Solid State Ionics) from the Ministry of Education, Science, Sports, and Culture.

REFERENCES

1. J. G. Bednorz and K. A. Muller, *Z. Phys. B* **64,** 189 (1986).
2. K. Kishio, K. Kitazawa, S. Kanbe, I. Yasuda, N. Sugii, H. Takagi, S. Uchida, K. Fueki, and S. Tanaka, *Chem. Lett.* 429 (1987).
3. M. K. Wu, J. R. Ashburn, C. J. Torng, P. H. Hor, R. L. Meng, L. Gao, Z. J. Huang, Y. Q. Wang, and C. W. Chu, *Phys. Rev. Lett.* **58,** 908 (1987).
4. H. Maeda, Y. Tanaka, M. Fukutomi, and T. Asano, *Jpn. J. Appl. Phys.* **27,** L209 (1988).
5. R. J. Cava, A. Santro, D. W. Johnson Jr., and W. W. Rhodes, *Phys. Rev. B* **35,** 6716 (1987).
6. S. Uchida, T. Ido, H. Takagi, T. Arima, and Y. Tokura, *Phys. Rev. B* **43,** 7942 (1991).
7. J. B. Torrance, Y. Tokura, A. I. Nazzal, A. Bezinge, T. C. Huang, and S. S. P. Parkin, *Phys. Rev. Lett.* **61,** 1127 (1988).
8. T. B. Lindemer, J. F. Hunley, J. E. Gates, A. L. Sutton Jr., J. Boynestad, C. R. Hubbard, and P. K. Gallagher, *J. Am. Ceram. Soc.* **72,** 1775 (1989).
9. J. Shimoyama, J. Kase, T. Morimoto, J. Mizusaki, and H. Tagawa, *Physica C* **185–189,** 931 (1991).
10. A. Caneiro, D. Serafini, J. P. Abriata, J. Andrade, and J. A. Gamboa, *Solid State Commun.* **75,** 915 (1990).
11. D. Serafini, A. Caneiro, and J. P. Abriata, *Jpn. J. Appl. Phys.* **30,** L468 (1990).
12. Y. Idemoto and K. Fueki, *Jpn. J. Appl. Phys.* **29,** 2725 (1990).
13. F. A. Kröger, "*The Chemistry of Imperfect Crystals.*" North Holland, Amsterdam, 1974.
14. E. J. Opila and H. L. Tuller, *J. Am. Ceram. Soc.* **77,** 2727 (1994).
15. S. Nishiyama, N. Kieda, K. Shinozaki, M. Kato, and N. Mizutani, *J. Ceram. Soc. Jpn.* **97,** 1123 (1989).
16. J. B. Torrance, A. Bezinge, A. I. Nazzal, T. C. Huang, S. S. P. Parkin, D. T. Keane, S. J. LaPlaca, P. M. Horn, and G. A. Held, *Phys. Rev. B* **40,** 8872 (1989).
17. H. Kanai, T. Hashimoto, H. Tagawa, and J. Mizusaki, unpublished.
18. T. Hashimoto, T. Yoshida, H. Kanai, H. Tagawa, and J. Mizusaki, unpublished.
19. J. Mizusaki, H. Tagawa, K. Naraya, and T. Sasamoto, *Solid State Ionics* **49,** 111 (1991).
20. T. Hashimoto, R. Hirasawa, T. Yoshida, Y. Yonemura, H. Tanaka, J. Mizusaki, and H. Tagawa, *J. Phys. Chem. Solids* **56,** 777 (1995).
21. K. Kishio, J. Shimoyama, T. Hasegawa, K. Kitazawa, and K. Fueki, *Jpn. J. Appl. Phys.* **26,** L1228 (1987).
22. C. Wagner, *Prog. Solid State Chem.* **6,** 1 (1971).
23. M. W. Shafer, T. Penney, and B. L. Olson, *Phys. Rev. B* **36,** 4047 (1987).
24. C. Chillout, S. W. Cheong, Z. Fisk, M. S. Lehmann, M. Marezio, B. Morosin, and J. E. Schirber, *Physica C* **158,** 183 (1989).
25. for example, T. Kamiyama, F. Izumi, H. Asano, H. Takagi, S. Uchida, Y. Tokura, E. Takayama-Muromachi, M. Matsuda, K. Yamada, Y. Endoh, and Y. Hidaka, *Physica C* **172,** 120 (1990).
26. J. Mizusaki, Y. Mima, S. Yamauchi, and K. Fueki, *J. Solid State Chem* **80,** 102 (1989).
27. O. T. Sørensen, "*Nonstoichiometric Oxides.*" Academic Press, London, 1981.
28. R. A. Swallin, "*Thermodynamics of Solids.*" Wiley, New York, 1962.